

## Continuous cooling precipitation diagram of high alloyed Al–Zn–Mg–Cu 7049A alloy

Davit ZOHRABYAN<sup>1,2</sup>, Benjamin MILKEREIT<sup>1,2</sup>, Christoph SCHICK<sup>2</sup>, Olaf KESSLER<sup>1</sup>

1. Chair of Materials Science, University of Rostock, 18051 Rostock, Germany;

2. Polymer-Physics Group, University of Rostock, 18051 Rostock, Germany

Received 17 October 2013; accepted 15 April 2014

**Abstract:** The precipitation behaviour during cooling from solution annealing of high alloyed 7049A aluminium alloy was investigated, covering the complete cooling-rate-range of technical interest. This ranges from slow cooling rates close to equilibrium up to rates above complete supersaturation and is covering seven orders of magnitude in cooling rate (0.0005 to 5000 K/s). The continuous cooling precipitation behaviour of 7049A alloy was recorded by combining different differential scanning calorimetry (DSC) techniques and microstructure analysis by SEM and Vickers hardness testing. The high alloyed, high strength and quench sensitive wrought aluminium alloy 7049A was investigated during quenching from solution annealing by conventional DSC in the cooling rate range of 0.0005 to 4 K/s. In this range at least two exothermal precipitation reactions were observed: a high temperature reaction in a narrow temperature interval of 450–430 °C, and a low temperature reaction in a broad temperature interval down to about 200 °C. Intensities of both reactions decreased with increasing cooling rate. Quenching from solution annealing with rates up to 1000 K/s was investigated by differential fast scanning calorimetry (DFSC) and the differential reheating method (DRM). A critical quenching rate to suppress all precipitation reactions of 100–300 K/s was been determined.

**Key words:** differential scanning calorimetry (DSC); differential fast scanning calorimetry (DFSC); 7049A alloy; differential reheating method; continuous cooling precipitation

### 1 Introduction

Age hardening is the most important heat treatment to strengthen aluminium alloys. It consists of solution annealing, quenching and ageing. Solution annealing and quenching result in a supersaturated solution, from which fine precipitates are formed during ageing. These fine precipitates hinder dislocation gliding and thereby increase the strength of aluminium alloys [1]. If quenching occurs too slow, coarse precipitates may already form during cooling. These precipitates usually are too big to hinder dislocation gliding effectively. Therefore, they reduce the strength after ageing. Several investigations of the precipitation processes during ageing exist, but only few investigations involve the precipitation processes during cooling from solution annealing [2–13]. The critical cooling rate (CCR) [10–12] gives information about the slowest cooling rate where all precipitation reactions are suppressed completely

[10,11]. After cooling aluminium alloys at the CCR or even faster (overcritical cooling) the maximum hardness after ageing was achieved [11]. Depending on the type of aluminium alloy and composition, the CCR can change dramatically (for 6xxx aluminium alloys typically from some 0.1 K/s to some 100 K/s) [11]. The CCR is commonly obtained from continuous cooling precipitation (CCP) diagrams [10,11]. However, CCP diagrams for aluminium alloys are hardly available. The common recording procedures for steels are not usable and only few other experimental procedures exist. One possibility for recording CCP diagrams of aluminium alloys is given by differential scanning calorimetry (DSC) [8,10–12,14,15]. Due to the fact that modern DSC still has a limited cooling rate range (typically below 10 K/s), aluminium alloys which have CCRs higher than the cooling rate range achievable by the device cannot be studied [11,16]. The problem may be solved by the recently developed differential fast scanning calorimetry (DFSC) [17–19] reaching cooling rates up to 10<sup>6</sup> K/s.

## 2 Experimental

Wrought aluminium alloy EN AW-7049A (Al–8.2Zn–2.9Mg–1.9Cu) has a high content of alloying elements and the precipitation heat is expected to be large. Further this alloy is expected to have a high critical cooling rate. It is therefore a good candidate for the investigation of precipitation behaviour over a broad range of cooling rates. This alloy is used in various load carrying parts of aircrafts. The alloy has been available as an extruded profile 50 mm (diameter). EN AW-1050 commercially pure aluminium with an aluminium mass fraction of more than 99.5%, was used as reference material. No precipitation reactions were detectable for this material in the temperature range of interest. The compositions of the alloys are given in Table 1.

**Table 1** Alloying elements of used aluminium alloys (mass fraction, %)

Alloy	Si	Fe	Cu	Mn	Mg	Cr	Zn	Ti
EN AW-1050	0.09	0.32	0.002	0.004	0.001	0.001	0.01	0.004
EN AW-7049A	0.25	0.35	1.90	0.20	2.90	0.22	8.2	0.10

The samples were solution annealed and cooled in three different types of commercial differential scanning calorimeters (DSC), in two innovative differential fast scanning calorimeters (DFSC) and in a quenching dilatometer. The conditions for heat treatment were provided below: Heating was carried out at 0.83 K/s; Solution annealing temperature was 470 °C; Solution annealing time was 30 min for conventional DSC and 15 min for DFSC.

The quenching step was varied from very slow (near to equilibrium) up to very fast rates where precipitation was expected to be suppressed. Slow cooling experiments from 0.0005 K/s to 0.025 K/s were executed in a heat flow type DSC Setaram 121 [10]. Sample dimensions were about 6 mm (diameter)×22 mm (mass of about 1850 mg). Samples were placed in standard aluminium crucibles. The cooling rates in the intermediate range from 0.083 K/s to 0.5 K/s were performed employing the heat flow type Mettler Toledo DSC 823, 822. The optimal samples for these rates and this device had typical dimensions of about 5.4 mm in diameter and 1.4 mm in height, which results in a sample mass of approximately 96 mg [10]. The samples were placed in standard aluminium crucibles. The fastest DSC which was used in the range from 0.6 K/s to 4 K/s was the Perkin Elmer Pyris 1 DSC. This type of DSC had a typical power compensation scheme. The sample had dimensions of 4 mm in diameter and 1 mm in height.

The dimensions result in a sample mass of about 30 mg. These samples were placed inside pure aluminium crucibles. Excess specific heat capacity was calculated from all experiments and evaluation was performed according to the results by MILKEREIT et al [10]. It is important to mention that for the excess specific heat capacity calculation baseline experiments have to be performed each time. In this case the reference material mentioned above was used in both furnaces of the device. Thereby, the difference between specific heat capacity of EN AW 7049A and EN AW 1050 was calculated.

The quenched DSC samples were afterwards naturally aged in T4 mode. Natural ageing was performed at room temperature (24 °C) for 30 d. The purpose of this procedure was hardness investigation as well as metallographic tests for comparison with the data acquired from different DSC's. Then the samples were placed into epoxy resin, ground, polished and etched. Light microscopy and scanning electron microscopy (SEM) analyses were performed with the samples obtained from the various DSC devices. When metallographic screening of the samples was finalized, the samples were subjected to hardness analysis. Each sample was tested total five indentations HV<sub>1</sub> within various areas. Calculation of the hardness was performed by averaging the values.

Even faster quenching rates up to 1000 K/s have been realised in a differential fast scanning calorimeter DFSC Mettler Toledo Flash as well as in self designed chip DFSC [19]. Unfortunately, these devices have a low sensitivity in the interesting quenching rate region of some 10 to some 100 K/s. Therefore, a new method, called differential reheating method (DRM) has been developed [20]. This method based on the idea that precipitates formed during cooling can also be characterized by their dissolution during following reheating. Reheating can be realised with faster rates in the optimal sensitivity range of the devices. DFSC samples are very small, and typical edge length is 100 µm. Solution annealing has been performed at the same temperature as mentioned above, but the solution annealing duration has been reduced to 15 min due to the small sample size. Quenching rates between 0.125 K/s and 2000 K/s have been investigated, namely, a broad overlap between DSC and DFSC has been realised. Reheating rates amounted 1000 K/s, and overcritical quenching as a reference has been performed with 8000 K/s. Because DFSC samples are too small for common microstructure investigations and hardness test, high quenching rates have also been realised in a quenching dilatometer Bähr 805A/D. Sample dimensions are 4–5 mm (diameter)×10 mm and quenching rates of some 100 K/s can be achieved. Altogether, quenching rates from

0.0005 K/s to some 1000 K/s, i.e. seven orders of magnitude, have been investigated.

### 3 Results and discussion

The excess specific heat capacity of aluminium alloy EN AW 7049A during cooling with rates from 0.001 K/s to 4 K/s is demonstrated in Fig. 1. This cooling rate range has been covered by the three conventional DSC devices Setaram 121 DSC, Mettler-Toledo 823 DSC and Perkin-Elmer Pyris 1 DSC. The slowest cooling rates of 0.0005 K/s and 0.001 K/s were hard to evaluate. From 0.025 K/s to 4 K/s the excess specific heat capacity shows at least two overlapping main peaks. The first relative sharp peak (high temperature precipitation) starts at about 450 °C for low cooling rates. With increasing cooling rate, it shifts to lower temperatures. The second broad peak (low temperature precipitation) is characterized by a slowly decreasing excess heat capacity down to a temperature of about 175 °C at 0.001 K/s. At cooling rates faster than 3 K/s separation of the two main peaks is not possible. They finish at 225–250 °C for 4 K/s.

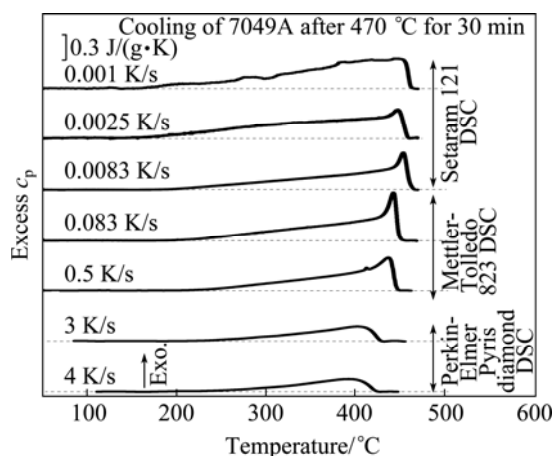


**Fig. 1** Excess specific heat capacity of aluminium alloy EN AW-7049A during cooling with rates from 0.001 K/s to 4 K/s

The areas under the precipitation peaks become smaller with increasing cooling rate. They give the precipitation heat as plotted in Fig. 2 as the sum of all precipitations. The precipitation heat decreases continuously also at such cooling rates, where the DSC device has been changed. This proves reliability of the experimental results. For low cooling rates, the precipitation heat amounts about 50 J/g. This precipitation heat is large compared to other aluminium alloys (e.g. 6xxx wrought alloys [11]), due to the high alloying element content in EN AW-7049A. With increasing cooling rate, the precipitation heat decreases down to 10–15 J/g at 4 K/s, namely, the critical cooling rate is significantly higher. A cooling rate of 4 K/s is the

upper limit of conventional DSC in the configuration used in our lab. Therefore, the precipitation behaviour during cooling has been further investigated by differential fast scanning calorimetry (DFSC) and the differential reheating method up to 5000 K/s.

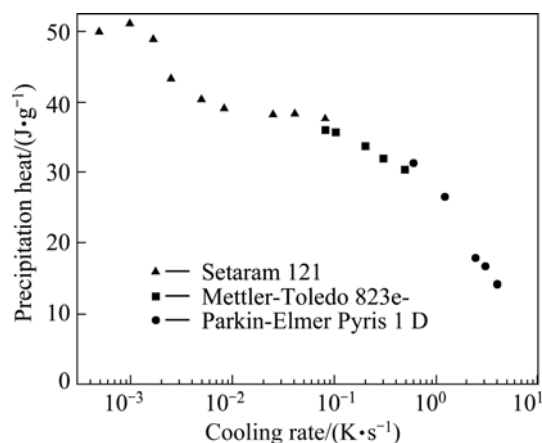


**Fig. 2** Precipitation heat of aluminium alloy EN AW 7049A during cooling with rates from 0.0005 K/s to 4 K/s

The differential heat flow of aluminium alloy EN AW-7049A during reheating after cooling with rates from 0.125 K/s to 2000 K/s is demonstrated in Fig. 3. Cooling rates of 0.125 K/s to 4 K/s overlap with experiments in conventional DSC. They show relative large differential heat flow peaks and agree with direct measurements during cooling. With increasing cooling rate, the differential heat flow during reheating decreases. The area under the differential heat flow peaks has been evaluated in Fig. 4 for seven different sets of reheating experiments. Because the exact sample mass is not known, the peak area is given in arbitrary units. Due to demanding preparation of the very small DFSC samples and due to possible chemical inhomogeneities among

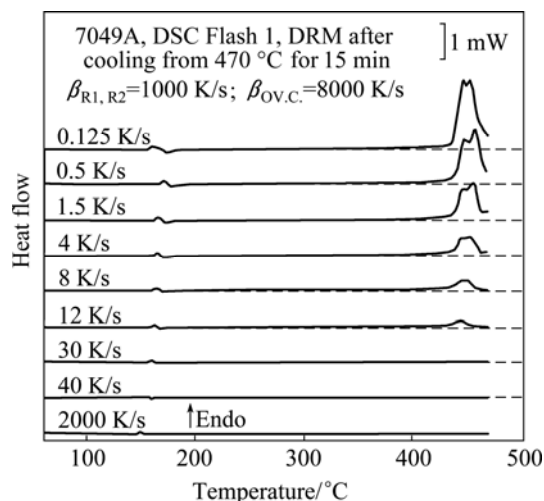


**Fig. 3** Differential heat flow of aluminium alloy EN AW-7049A during reheating after cooling with rates from 0.125 K/s to 2000 K/s

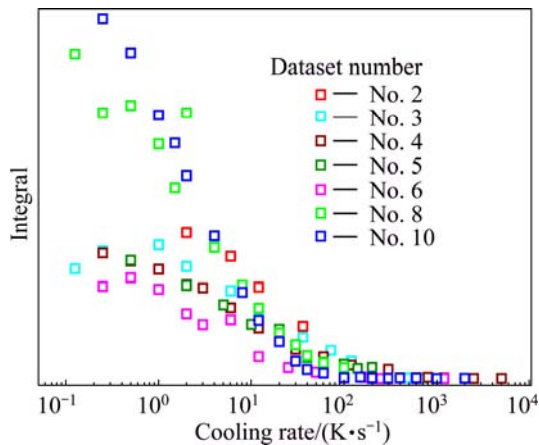


**Fig. 4** Integration of differential heat flow of aluminium alloy EN AW 7049A during reheating after cooling with rates from 0.125 K/s to 5000 K/s

the very small DFSC samples, absolute peak areas differ relatively strong. But the important result is that for all seven sets of reheating experiments, the peak areas reach zero level at very similar cooling rates, namely, DFSC experiments are reproducible. The peak area reaches zero level at 100–300 K/s, namely, the critical cooling rate of aluminium alloy EN AW 7049A is 100–300 K/s. The high critical cooling rate is due to the high amount of alloying elements in aluminium alloy EN AW 7049A.

Because of the cooling rate overlap between DSC and DFSC, the peak areas of DFSC can be normalised by the peak areas of corresponding DSC tests. Figure 5 summarises the precipitation heat of all DSC and DFSC experiments in the cooling rate range from 0.0005 K/s to 2000 K/s, i.e. an investigated cooling rate range of seven orders of magnitude. Precipitation heat decreases continuously with increasing cooling rate down to the critical cooling rate of 100–300 K/s. Opposite, the hardness after ageing T4 increases from about HV<sub>1</sub> 60 at

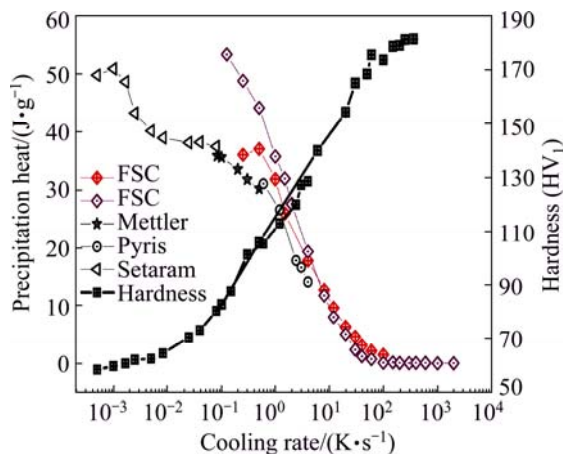


**Fig. 5** Precipitation heat and hardness of aluminium alloy EN AW-7049A after cooling with rates from 0.0005 K/s to 2000 K/s and after ageing T4

0.0005 K/s to about HV<sub>1</sub> 180 at 300 K/s. All alloying element atoms lost in coarse precipitates during slow cooling cannot participate in strengthening by fine precipitates during ageing. The high hardness of HV<sub>1</sub>180 in the T4 state after overcritical cooling is due to the high amount of alloying elements in aluminium alloy EN AW-7049A.

Figure 6 demonstrates microstructures of aluminium alloy EN AW 7049A (light microscopy) after cooling at rates of 0.001, 0.08 and 0.6 K/s, respectively. All images show three types of precipitates. The first type is large (a few 10 μm) precipitates in irregular shape (red circles). Their sizes do not depend on cooling rate, namely, they are primary precipitates. The second type is polygonal shaped precipitates (green circle). Their sizes decrease with increasing cooling rate from about 10 μm at 0.001 K/s to about 1 μm at 0.6 K/s. The third type is needle-shaped precipitates (blue circles). Their lengths

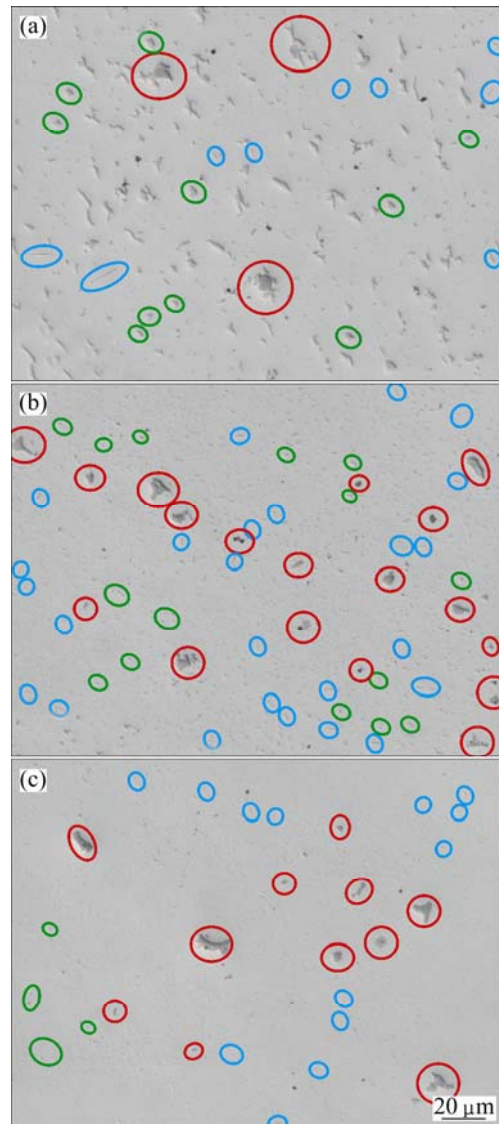


**Fig. 6** Optical microstructure of aluminium alloy EN AW-7049A: (a) Cooling rate of 0.0016 K/s; (b) Cooling rate of 0.08 K/s; (c) Cooling rate of 0.6 K/s

decrease with increasing cooling rate from about 10  $\mu\text{m}$  at 0.001 K/s to about 1  $\mu\text{m}$  at 0.6 K/s. After a cooling rate of 0.6 K/s, the last two types are hardly visible although the precipitation heat still amounts about 30 J/g (Fig. 5). A large number of smaller precipitates must be present and will be investigated by scanning electron microscopy.

Figure 7 shows the SEM images of aluminium alloy EN AW-7049A after cooling with rates of 0.1, 0.5 and 4 K/s. Polygonal and needle-shaped secondary precipitates are also visible in SEM images. Their chemical composition was measured by energy dispersive X-ray analysis. Both of them contained large amounts of zinc, magnesium and copper. Due to relative slow cooling, these precipitates are assumed to be equilibrium phases like  $\eta$ -Zn<sub>2</sub>Mg and S-Al<sub>2</sub>CuMg. Their sizes decrease with increasing cooling rate from a few  $\mu\text{m}$  at 0.1 K/s to a few 0.1  $\mu\text{m}$  at 4 K/s.

The precipitation start and end temperatures of the overall reaction as well as the intersection between high-temperature (HTR) and low-temperature reaction (LTR) were evaluated from the conventional DSC-measurements. The corresponding time–temperature data

points were plotted in a time–temperature diagram. Figure 8 shows the resulting continuous cooling precipitation diagram of EN AW-7049A after solution annealing at 470 °C for 30 min and the chemical compositions as listed in Table 2. The time scale is scaled logarithmic. The critical cooling rate range detected by DFSC is identified by a hatched cross pattern.

**Table 2** Chemical composition of EN AW-7049A (mass fraction, %)

Si	Fe	Cu	Mn
0.25	0.35	1.90	0.20
Mg	Cr	Zn	Ti
2.90	0.22	8.2	0.10

## 4 Conclusions

The exothermal heat flow from quench-induced precipitation in wrought aluminium alloy EN AW-7049A during cooling was investigated by measuring excess specific heat capacity curves with DSC over a cooling rate range from 0.0005 K/s to some 1000 K/s, i.e. seven

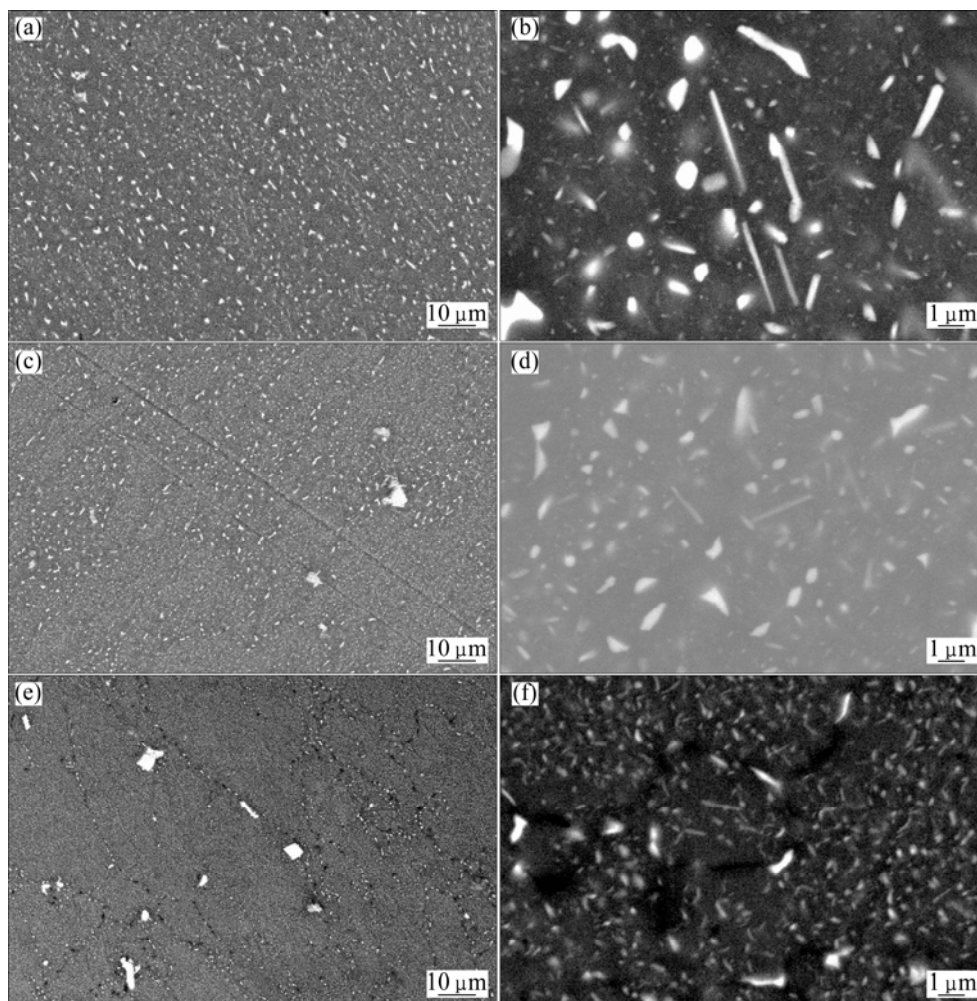


**Fig. 7** SEM images of aluminium alloy EN AW-7049A: (a, b) Cooling rate of 0.1 K/s; (c, d) Cooling rate of 0.5 K/s; (e, f) Cooling rate of 4 K/s

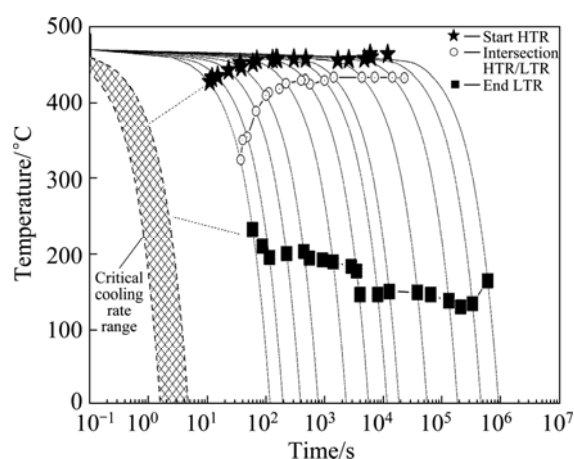


**Fig. 8** Continuous cooling precipitation diagram of EN AW-7049A after solution annealing at 470 °C for 30 min

orders of magnitude. The influence of the cooling rate on the precipitation behaviour was described. The results show that there are at least two different quench-induced precipitation reactions occurring during cooling in specific cooling rate ranges. The microstructural analysis points on the existence of equilibrium  $\eta$ -Zn<sub>2</sub>Mg and S-Al<sub>2</sub>CuMg phase, at least for low cooling rates. Premature precipitation during quenching from solution annealing decreases the hardness after ageing. Differential fast scanning calorimetry was applied to cover the cooling rate range needed for high alloyed materials. A new methodology, called differential reheating method, was applied for differential fast scanning calorimetry (DFSC). The critical cooling rate for the quench sensitive EN AW-7049A alloy was determined as 100–300 K/s.

## Acknowledgement

The authors acknowledge funding of this work by a scholarship of the German State of Mecklenburg-Vorpommern via University of Rostock, Interdisciplinary Faculty.

## References

- [1] POLMEAR I J. Light alloys [M]. Oxford: Butterworth-Heinemann, 2006.
- [2] CAVAZOS J L, COLAS R. Quench sensitivity of a heat treatable aluminum alloy [J]. *Materials Science and Engineering A*, 2003, 363: 171–178.
- [3] LI H Y, GENG J F, ZHENG Z Q, WANG C J, SU Y, HU B. Continuous cooling transformation curve of a novel Al–Cu–Li alloy [J]. *Transactions of Nonferrous Metals Society of China*, 2006, 16: 1110–1115.
- [4] LI H Y, ZHAO Y K, TANG Y, WANG X F. Determination and application of cct diagram for 6082 aluminum alloy [J]. *Acta Metallurgica Sinica*, 2010, 46: 1237–1243.
- [5] LI H Y, ZHAO Y K, TANG Y, WANG X F, DENG Y Z. Continuous cooling transformation curve for 2A14 aluminum alloy and its

application [J]. *The Chinese Journal of Nonferrous Metals*, 2011, 21(5): 968–974. (in Chinese)

- [6] LI P Y, XIONG B Q, ZHANG Y A, LI Z H, ZHU B H, WANG F, LIU H W. Quench sensitivity and microstructure character of high strength AA7050 [J]. *Transactions of Nonferrous Metals Society of China*, 2012, 22: 268–274.
- [7] DESCHAMPS A, TEXIER G, RINGEVAL S, DELFAUT-DURUT L. Influence of cooling rate on the precipitation microstructure in a medium strength Al–Zn–Mg alloy [J]. *Materials Science and Engineering A*, 2009, 501: 133–139.
- [8] MILKEREIT B, BECK M, REICH M, KESSLER O, SCHICK C. Precipitation kinetics of an aluminium alloy during Newtonian cooling simulated in a differential scanning calorimeter [J]. *Thermochemica Acta*, 2011, 522: 86–95.
- [9] MILKEREIT B, JONAS L, SCHICK C, KESSLER O. Das kontinuierliche zeit-temperatur-ausscheidungs-diagramm einer aluminiumlegierung EN AW-6005A [J]. *HTM Journal of Heat Treatment and Materials*, 2010, 65: 159–171.
- [10] MILKEREIT B, KESSLER O, SCHICK C. Recording of continuous cooling precipitation diagrams of aluminium alloys [J]. *Thermochemica Acta*, 2009, 492: 73–78.
- [11] MILKEREIT B, WANDERKA N, SCHICK C, KESSLER O. Continuous cooling precipitation diagrams of Al–Mg–Si alloys [J]. *Materials Science and Engineering A*, 2012, 550: 87–96.
- [12] von BARGEN R, KESSLER O, ZOCH H W. Continuous-cooling-transformation diagrams of the aluminium alloys EN AW-7020 and EN AW-7050 [J]. *HTM-Journal of Heat Treatment and Materials*, 2002, 62(6): 285–293. (in German)
- [13] ZAJAC S, BENGTTSSON B, JÖNSSON C, ISAKSSON A. Quench sensitivity of 6063 and 6082 aluminium alloys [C]//International Aluminum Extrusion Technology Seminar. Chicago: Aluminum Extruders Council, 2000: 73–82.
- [14] HERDING T, KESSLER O, HOFFMANN F, MAYR P. An approach for continuous cooling transformation (CCT) diagrams of aluminium alloys [C]//GREGSON P J, HARRIS S J. 8<sup>th</sup> International Conference on Aluminium Alloys. Cambridge, UK: Trans Tech Publications Ltd, 2002: 869.
- [15] KESSLER O, VON BARGEN R, HOFFMANN F, ZOCH H W. Continuous cooling transformation (CCT) diagram of aluminum alloy Al–4.5Zn–1Mg [C]//POOLE W J, WELLS M A, LLOYD D J. 10<sup>th</sup> International Conference on Aluminium Alloys 2006, Pts 1 and 2. Vancouver, Canada: Trans Tech Publications, 2006: 1467–1472.
- [16] MILKEREIT B, SCHICK C, KESSLER O. Continuous cooling precipitation diagrams depending on the composition of aluminum-magnesium-silicon alloys [C]//KUMAI S, UMEZAWA O, Y. TAKAYAMA, TSUCHIDA T, SATO T. 12. International Conference on Aluminium Alloys. Yokohama: The Japan Institute of Light Metals, 2010: 407–412.
- [17] ADAMOVSKY S A, MINAKOV A A, SCHICK C. Scanning microcalorimetry at high cooling rate [J]. *Thermochemica Acta*, 2003, 403: 55–56.
- [18] MINAKOV A A, SCHICK C. Ultrafast thermal processing and nanocalorimetry at heating and cooling rates up to 1 MK/s [J]. *Review of Scientific Instruments*, 2007, 78: 073902.
- [19] ZHURAVLEV E, SCHICK C. Fast scanning power compensated differential scanning nano-calorimeter: Part 1. The device; Part 2: Heat capacity analysis [J]. *Thermochemica Acta*, 2010, 50: 1–21.
- [20] ZOHRABYAN D, MILKEREIT B, KESSLER O, SCHICK C. Precipitation enthalpy during cooling of aluminum alloys obtained from calorimetric reheating experiments [J]. *Thermochemica Acta*, 2012, 529: 51–58.

# 高合金化 Al-Zn-Mg-Cu 系 7049A 合金的 连续冷却析出图

Davit ZOHRABYAN<sup>1,2</sup>, Benjamin MILKEREIT<sup>1,2</sup>, Christoph SCHICK<sup>2</sup>, Olaf KESSLER<sup>1</sup>

1. Chair of Materials Science, University of Rostock, 18051 Rostock, Germany;

2. Polymer-Physics Group, University of Rostock, 18051 Rostock, Germany;

**摘要:** 研究了所有有技术价值的冷却速率范围内 7049A 铝合金的析出行为。冷却速率从接近平衡冷却时的慢速条件变化到形成完全超饱和固溶体的高速率, 跨越了 7 个数量级(0.0005 到 5000 K/s)。7049A 铝合金连续冷却析出行为采用差热分析(DSC)、扫描电镜(SEM)和维氏硬度测量相结合的方法记录。冷却速率在 0.0005 到 4 K/s 时, 对高合金化、高强度和高淬火敏感性的变形铝合金 7049A 从固溶温度下的淬火析出行为采用传统的 DSC 方法研究。在此冷却速率范围内, 至少观察到了两个放热反应: 一个是在很窄的温度区间 430~450 °C 内的高温反应; 另外一个是最小到 200 °C 且范围很宽的低温反应。这两个反应的强度随着冷却速率的增高而降低。采用快速差热分析(DFSC)和差分再加热方法(DRM)对合金淬火冷却速率从慢速到数千 K/s 时的析出行为进行了研究。该合金不析出沉淀相时的临界淬火速率为 100~300 K/s。

**关键词:** 差示扫描量热法; 快速差热分析; 7049A 合金; 微分加热方法; 连续冷却析出

(Edited by Hua YANG)